Review of aeronautical fatigue and structural integrity investigations in the Netherlands during the period March 2021 - March 2023

TU Delft

Review of aeronautical fatigue and structural integrity investigations in the Netherlands during the period March 2021 - March 2023

R.C. Alderliesten

Abstract

This report is a review of the aeronautical fatigue and structural integrity activities in the Netherlands during the period March 2021 to March 2023. The review is the Netherlands National Delegate's contribution to the 38th Conference of the International Committee on Aeronautical Fatigue and Structural Integrity (ICAF) in Delft, The Netherlands, on 26 to 29 June 2023, and published on the ICAF website in June 2023.

An electronic version of this review is available at http://repository.tudelft.nl/.

TU Delft

Table of Contents

Abbreviations

AE	Acoustic Emission
CA	Constant Amplitude
CFRP	Carbon fibre reinforced polymer composites
DCB	Double Cantilever Beam
DIC	Digital Image Correlation
FCG	Fatigue Crack Growth
FE	Finite Element
FOS	Fibre Optic Sensing
LEFM	Linear Elastic Fracture Mechanics
POF	Probability of Failure
PROF	PRrediction Of Fatigue in engineering alloys
QF	Quantitative Fractography
RNLAF	Royal Netherlands Air Force
SERR	Strain Energy Release Rate
SHM	Structural Health Monitoring
SIF	Stress Intensity Factor
TRL	Technology Readiness Level
UD	Unidirectional
VA	Variable Amplitude

1. Introduction

The present report provides an overview of the work and research performed in the Netherlands in the field of aeronautical fatigue and structural integrity during the period from March 2021 until March 2023. The subjects in this review come from the following contributors:

- Delft University of Technology (TU Delft)
- GKN Aerospace-Fokker (GKN Fokker)
- Netherlands Aerospace Centre (NLR)
- Royal Netherlands Air Force (RNLAF)
- University of Twente (UT)

Additionally, collaborative work between the NLR and the Defence Science and technology Group (DST-G) of Australia, and between TU Delft and various European universities and institutes is included.

The names of the principal investigators and their affiliations are provided at the start of each subject. The format and arrangement of this review is similar to that of previous national reviews.

2. Metal Fatigue

2.1. The physics of energy dissipation in fatigue crack growth and plasticity

Jesse van Kuijk, Hongwei Quan, René Alderliesten (TU Delft)

Two PhD dissertations were successfully defended recently where both the fatigue crack growth process was subject of scrutiny. The first study by Hongwei Quan, took the fundamental principles from physics in analysing the process, particularly focussing on the strain energy dissipation in crack tip plasticity [1].

Hongwei postulated that at any instance in the fatigue crack growth test, the following energy balance holds

$$\dot{W} = \dot{U}_a + \dot{U}_{pl} + \dot{U}_e \quad (1)$$

where the change in work applied $\dot{W}$ is equal to the sum of the change in fracture surface energy dissipated in formation of new surfaces, the energy dissipation in plasticity and the variation in elastic energy stored. When integrating equation (1) over entire cycles, the discrete form is obtained:

$$\frac{dW}{dN} = \frac{dU_a}{dN} + \frac{dU_{pl}}{dN} + \frac{dU_e}{dN} \quad (2)$$

Quan studied through combining numerical simulations with experimental testing how these different components relate to the discrete crack increments per cycle da/dN. This method of complementing the experiment with numerical simulation was necessary, because the quantities of energy dissipation through new fracture surface formation, and the variation in elastic energy stored is generally too small to measure. Through this analysis, it was observed that the crack growth rate da/dN has only a straightforward relationship with the fracture surface energy dissipated through formation of new fracture surfaces, while the relationship with the plastic energy dissipation an the variation in elastic energy stored exhibits apparent stress ratio effects, see Figure 1.

Quan explained in his dissertation and corresponding paper [2] that this relationship with the fracture surface energy dissipation is likely only affected by the different between the true fracture surface area caused by shear lip formation and fracture surface roughness, and the projected fracture plane subject in the definition of da/dN.

Investigating whether this energy balance of equations (1) and (2) also hold for adhesively bonded interfaces subject to mode I fatigue loading, demonstrated that the equations are correct, but that the absolute quantities between the individual terms differ.

The second dissertation, by Jesse van Kuijk [3] continued with this energy balance, developing a description for constant amplitude (CA) loading in which the individual components are quantified through describing the dissipation processes. Following the hypothesis by Quan, Van Kuijk expressed the fracture surface formation relative to the projected plane described by da/dN through two correction parameters for respectively the shear lip formation, i.e $\sqrt{2}$ for the portion of fracture under 45° shear angle, and for the roughness, through normalizing by a reference roughness at the start of fracture. Additionally, he demonstrated how for small cracks, the commonly used crack length is an incomplete measure for the fracture area, and that frequently reported mismatch between long crack data and small crack problems, easily can be explained by the incomplete nature o the crack length as descriptive parameter.

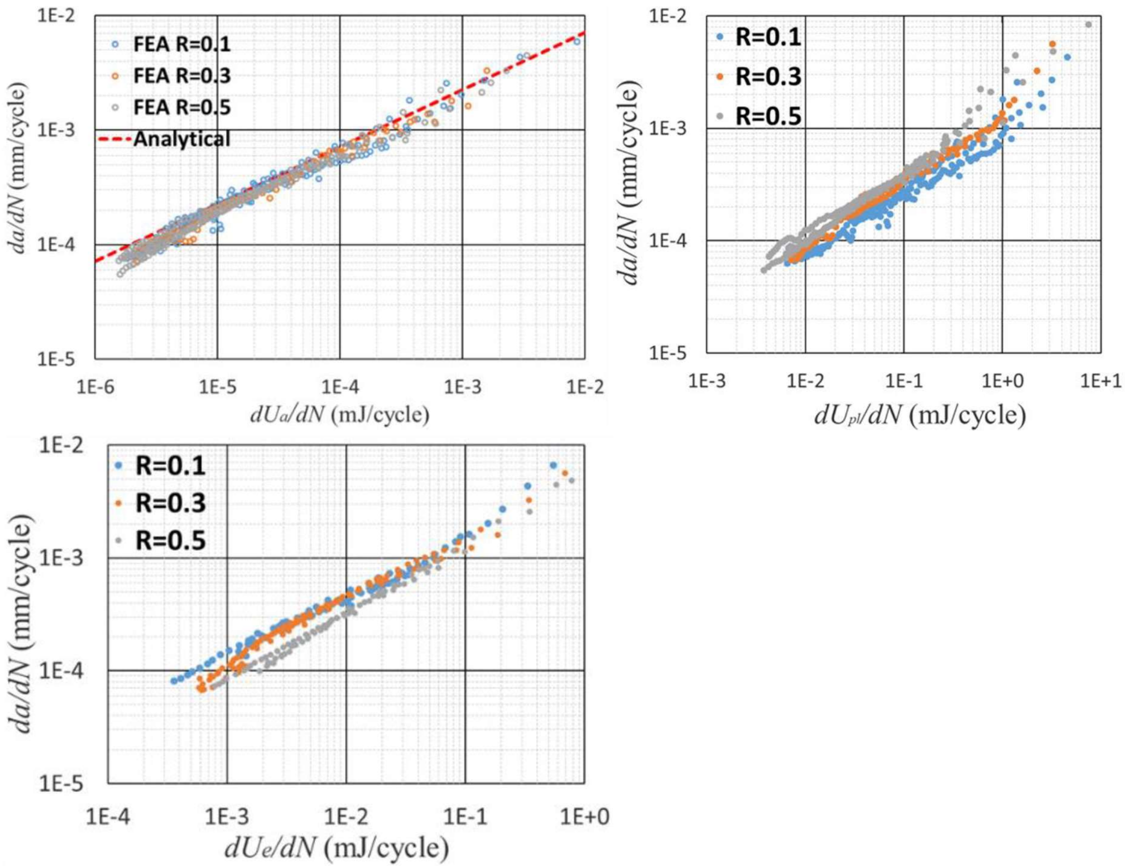

Figure 1 The correlation between the crack growth rate da/dN and the three components of equation (2); a unique and straightforward relation with dU_a/dN is observed, while the relationship with dU_{pl}/dN and dU_e/dN exhibits an apparent stress ratio effect.

The plastic energy dissipation was described through assuming Irwin's plastic zone as cylindrical volume through the thickness, which as crescent volume increases with crack growth. Assuming a relationship for the average strain energy density within the plastic volume, extracted from experiments on various alloys.

Van Kuijk observed that the energy balance of equation (2) cannot be used as prediction model, because the crack growth rate cancels out. In other words, equation (1) and (2) describe the instantaneous balance of dissipating processes, not how many times that process can be repeated. Taking another concept from physics, the analogy with a sliding box, Van Kuijk formulated a method to relate the work applied in fatigue loading to the dissipation of the energy balance.

Van Kuijk was able to predict the crack propagation in a centre-crack tension plate, while using only mechanical properties as input. The output was the crack growth curve, and derived from that he could predict the corresponding Paris curve.

2.2. Prediction of fatigue in engineering alloys – part 2(PROF-2)

Emiel Amsterdam (Netherlands Aerospace Centre NLR)

The PROF-2 project is a five year Public Private Partnership between NLR, C-TEC Constellium Technology Center, Lagerwey, RUAG, Korea Aerospace Industries, GKN Fokker, Airbus and the Ministry of Defense. The objective of the project is to develop a unified probabilistic fatigue life assessment framework. In PROF-2 knowledge of the fatigue crack growth rate (FCGR) of long and small cracks and their distribution will be gained and used to create a unified probabilistic fatigue life assessment framework that allows determining the life distribution of a structure for a given initial discontinuity size distribution or rogue flaw size. The proof of concept of the new theoretical framework from the initial PROF project will be extended to create a cycle-by-cycle model to predict VA crack growth for any given variable amplitude loading spectrum.

For positive stress ratios it was proven that the fatigue crack growth rate (da/dN) shows a power law relationship with the cyclic strain energy release rate (ΔG) over the maximum stress intensity factor (K_{max}):

$$\frac{da}{dN} = C\left(\frac{\Delta G}{K_{max}}\right)^n = C\left(\frac{(1-R^2)K_{max}}{E}\right)^n \qquad (3)$$

where *C* and *n* are material constants, *R* is the stress ratio and *E* the Young's modulus.

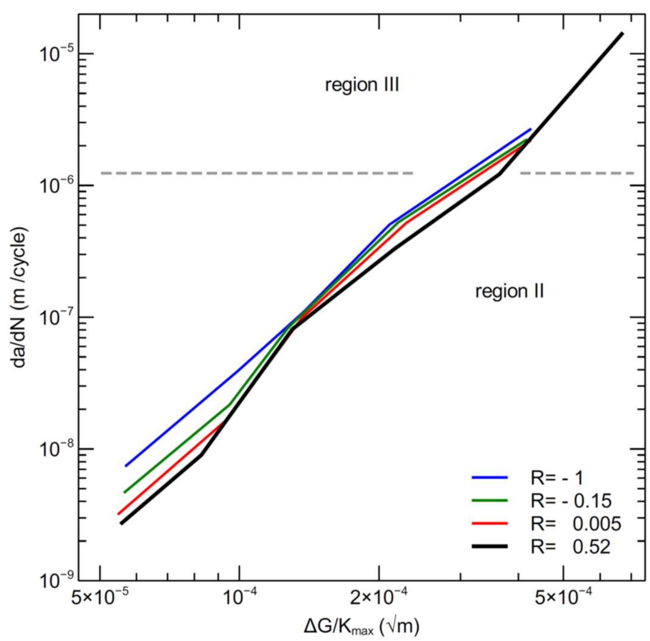

Figure 2 Fatigue crack growth rate of AA7075-T7351 as a function of the cyclic strain energy release rate (ΔG) over the maximum stress intensity factor (K_{max}) for different positive and negative stress ratios (R).

This equation is similar as the fatigue crack growth rate equation based on the effective stress intensity factor range (ΔK_{eff}) and the Young's modulus:

$$\frac{da}{dN} = C\left(\frac{(1-R^2)K_{max}}{E}\right)^n = C\left(\frac{(1+R)(1-R)K_{max}}{E}\right)^n$$

$$= C^*\left(\frac{(0.5+0.5R)\cdot\Delta K}{E}\right)^n \approx C^*\left(\frac{\Delta K_{eff}}{E}\right)^n \tag{4}$$

However, the effect of negative stress ratio was not characterized yet. In 2021 and 2022 fatigue crack growth rate tests were performed on middle tension specimens made from aluminium alloy (AA) 7075-T7351. The results show that there are still minor differences in the FCGR curve between R=0.52 and R=0.005 and that the negative stress ratio mainly affects the FCGR at the beginning and end of region II (see Figure 2). The FCGR is hardly affected by the stress ratio at a FCGR of 10^{-7} m/cycle.

2.3. The fatigue performance of aluminum alloy 7050 after treatment optimization for Cr(VI)-free anodizing processes for non-bonding applications

T. Janssen, J.M.M. de Kok, J.C.J. Hofstede (GKN Aerospace / Fokker Aerostructures, Papendrecht)

To comply with the European REACh legislation, GKN Fokker will move from using Chromic Acid Anodizing (CAA) as surface treatment for corrosion protection purposes for bonding applications as well as for non-bonding applications to a number of REACh compliant chemical surface treatment processes. For non-bonding applications, a selection of three alternative processes are developed: Phosphoric Sulfuric Acid Anodizing (PSA), Thin Film Sulfuric Acid Anodizing (TFSAA), and Tartaric Sulfuric Acid Anodizing (TSA). GKN Fokker develops and maintains its own material- and process specifications, in combination with which the company's own Strength Handbook provides applicable strength data.

The new, Cr(VI)-free processes were developed and qualified within the Materials & Processes department. In order to avoid part-specific certification efforts, the aim of the process qualification was to demonstrate a robust process that has at least equal performance as the CAA process. In this way, a gradual transition to the new treatment processes could be made, without the need for expensive drawing changes.

As part of the qualification of these processes, the results of an extensive fatigue testing campaign, performed with all relevant aluminum alloys, were evaluated in 2020-2021 to assess the effect of the combinations of pre-penetrant etching and post-penetrant anodizing on the fatigue properties. Unfortunately, aluminium alloy 7050 appeared to be rather sensitive to the applied process settings (pre-penetrant metal removal, alkaline etching step, acidic desmutting steps, etc.) and the PSA and TSA processes could not be qualified for application with this specific alloy in first instance.

After optimization of the treatment processes, mainly targeted to reduce End Grain Pitting (EGP) values, a new series of fatigue tests was performed. About 220 notched fatigue specimens with a relatively low stress concentration (Kt = 1.6) and standard manufacturing quality/surface roughness were subjected to cyclic tension-tension loading (R = 0.1) in both LT- and ST-grain direction. For LT-direction, tests were also performed with R = -1 (tension-compression).

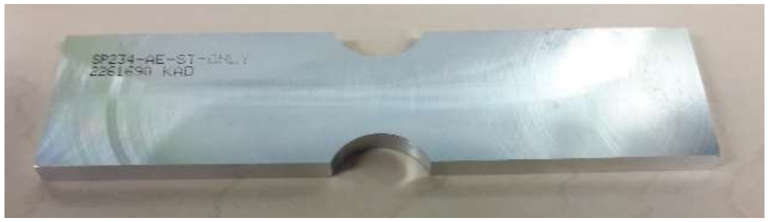

Figure 3 Typical example of a low Kt dogbone fatigue specimen

Specimens from plate alloys were extracted from the centre of the billet to represent worst-case grain structure, highest sensitivity to pickling and anodizing treatment and therefore worst-case fatigue properties.

On average, all processes showed slight improvements in measured EGP depths. However, the process optimizations resulted in significantly reduction of the maximum pit depths compared to the first test campaign. Anodic coating weights due to the anodizing process step were in the same range as before.

Fatigue tests were typically performed in the range of $10^3 – 10^7$ cycles. Again, the 7050-T745 plate alloy showed a clear transition from the 'Basquin-domain' towards a fatigue limit, regardless of the applied treatments. Test results were used for various curve-fitting procedures, including a power-law fit for the Basquin-domain, the staircase method for determination of the fatigue limit and a four-parameter Weibull equation covering the entire range of fatigue cycles to fracture. For each alloy-treatment combination, results from these the fitting processes are highly comparable and were useful for the comparative evaluation between the various processes. In addition, a statistical comparison between the data sets was performed, which assisted the evaluation when comparison of the fitted curves was inconclusive.

The results for PSA, TFSAA and TSA are evaluated and compared with the results obtained for the standard CAA process for each of the aluminum alloys tested, which showed that all 3 treatments including their respective pre-treatment processes (pickling, desmutting, etc.) performed equal or better than CAA.

The TFSAA process (subject to only minimum process optimization) performed only slightly better than in the previous campaign. The PSA and TSA processes improved significantly. The effect of the optimized (pre-) treatment steps for PSA and TSA were mainly observed in the domain of $10^5 – 10^7$ cycles, where improvements of 15-25% on treatment process knockdown factors (relative to the fatigue limit stress value of untreated material) were obtained with respect to the first test campaign.

Although the pre-penetrant treatment steps were Cr(VI) free and the sensitivity to the amount of metal removal was initially not expected, the various etching/pickling processes were shown to significantly affect the fatigue properties of especially the 7050-T7451 alloy, especially in the fatigue limit domain.

Recommendations on process solution parameters, immersion times and maximum allowed metal removal in order to limit the amount of end grain pitting to an acceptable level were transformed into treatment process optimizations that resulted in a successful qualification of three REACh-compliant surface treatment processes.

3. Composites

3.1. Vacuum infusion repair method of BMI composites supported by process simulation

Ronald Klomp, Wouter van den Brink (Royal Netherlands Aerospace Centre NLR)

The aim of this programme was to develop a robust and validated infusion repair procedure for Bismaleimide (BMI) composite structures for future aircraft. Process simulation is used to create a 'virtual repair' to improve the infusion and curing process of the BMI repair patch. The percentage of fiber reinforced materials (composites) in primary aircraft structures continues to grow. With this growth comes demand for continuous improvements in materials and manufacturing technology. Similar to more conventional composites, BMI composites are susceptible to damage and impacts from foreign objects. In case of such an impact or damage the structure needs to be repaired to achieve a close-to-original strength to enable continued use of the equipment.

The project on repair and simulation has proven to be very valuable to gain insight in the BMI material, process parameters and improvements of in the repair process. Manufacturing trials have been performed on various designs of infusion repairs including Twenco wireless process monitoring sensors – see Figure 4. With this sensor data the simulation tools developed on infusion and curing could be validated. Additionally, manufacturing trials were performed on partly transparent base material to monitor the infusion process optically. The developed repair method including process simulation has been successfully shown on the project-specific demonstrator wing box – see Figure 5. The repaired BMI wing box behaved very similar to the pristine panel which indicated a good repair process. Furthermore the numerical analyses tools were able to predict the repair process and test behaviour.

Figure 4.a: Repair layout with the new method

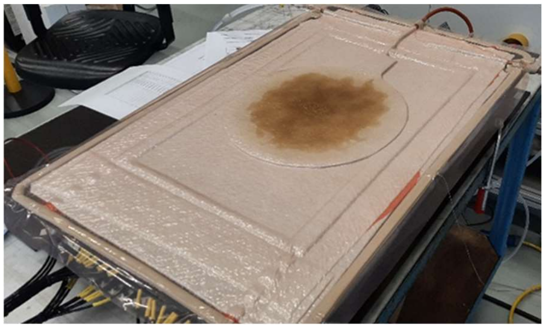

Figure 4.b: Cured repair.

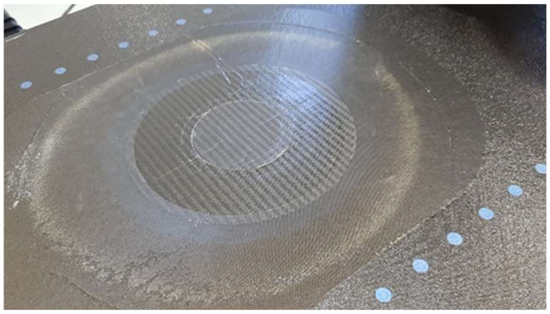

Figure 4.c: Final repaired panel.

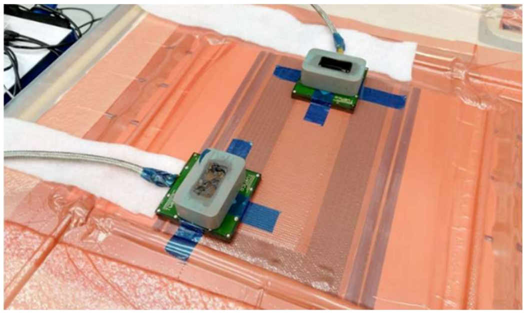

Figure 4.d: Twenco sensors used during infusion & curing.

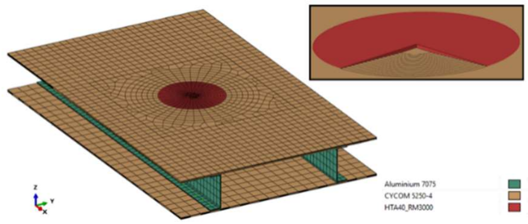

Figure 5.a: Model of the demonstrator wing box.

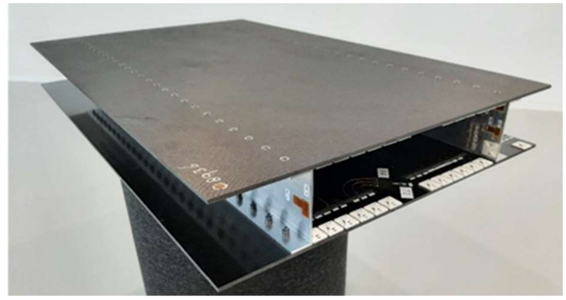

Figure 5.b: Assembled wing box.

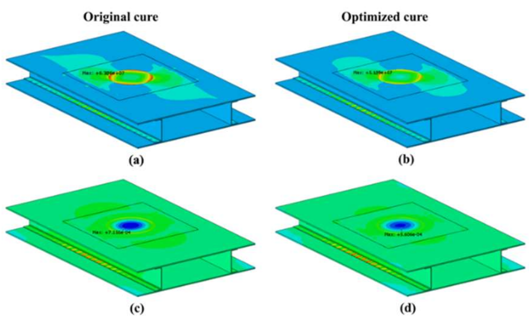

Figure 5.c: Curing simulation and improvements of the process.

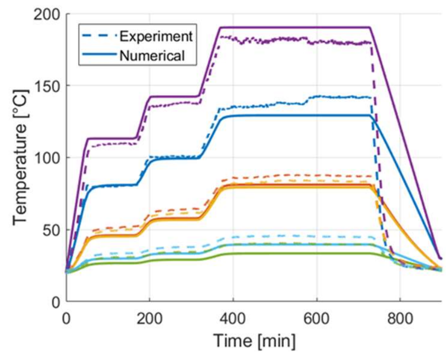

Figure 5.d: Comparison on numerical and experimental results.

3.2. From coupon to full-scale composite structure for fatigue of FRP composites

John-Alan Pascoe (TU Delft)

Over the past two years, a number of research projects have been carried out at TU Delft, attempting to bridge the gap between coupon testing and full scale structures for fatigue behaviour of fibre reinforced polymer composites. Within academia, there is a lot of fatigue testing of composites at the coupon level. However, it is difficult to generalise the results from these tests to the behaviour of full-scale components due to size and edge effects, and differences in active damage modes. These issues were explored in more depth during a presentation at the 1st Virtual European Conference on Fracture (recorded presentation: https://www.youtube.com/watch?v=sgjbxIZivYo) [4].

As part of his PhD research, Davide Biagini has been using acoustic emission (AE) due distinguish between different damage modes. In quasi-static compression after impact he was able to distinguish 3 distinct phases and identify that significant damage appears to already occur at approximately 80% of the final failure load [5]. The experimental dataset is publicly available via: https://doi.org/10.4121/21621381.v1. The next step is to investigate the damage evolution during fatigue after impact. Some preliminary findings were presented at ECF 22 [6], and further results will be show during ICAF 2023.

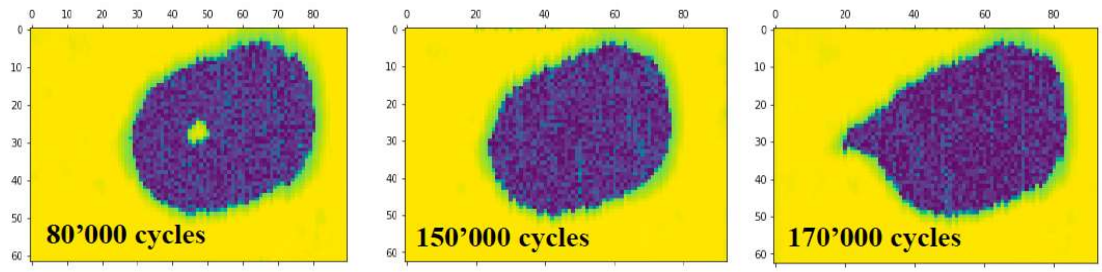

Figure 6 Ultrasonic C-scan at three stage of fatigue life. The initial growth appears to be inwards, first closing the undamaged cone, before outward growth occurs. Reproduced from. [6].

Figure 6 illustrates that simply measuring the width or total area of the delaminations detected by an ultrasonic scan is insufficient to fully characterise the damage growth. It seems likely that more sophisticated damage descriptors are needed to enable proper fatigue growth predictions.

In full-scale structures delaminations usually grow in 2D, planar, manner. However, the standard specimen geometries used to study delamination growth in the lab (e.g. double cantilever beam, DCB) induce one dimensional delamination growth. Only limited work has so far been done to investigate planar growth experimentally [7]. Therefore a new PhD project was started at TU Delft to develop new experimental methods for investigating this issue. This research is being conducted by Wenjie Tu, who will present the first results at ICAF 2023.

Mike van der Panne conducted an MSc thesis research into the effect of fibre orientation on fatigue driven delamination growth, the results of which were presented at ECF 22 [8]. A condensed view of this data is shown in Figure 7. Changing the fibre orientation at the interface results in a change in the fibre bridging / crack migration behaviour, which results in a shift in the Paris curve. This adds to the shift in the curve caused by fibre bridging [9].

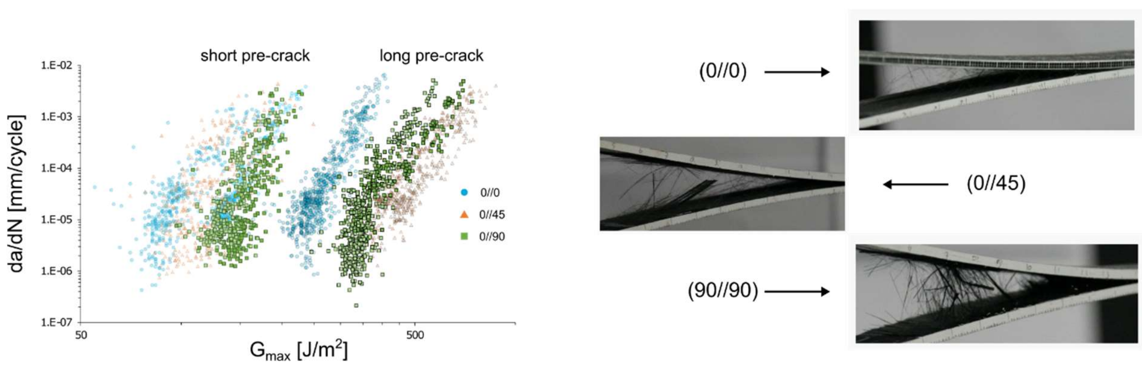

Figure 7 Effect of fibre orientation on delamination growth rate and fibre bridging behaviour, data previously presented in [8]

Finally, January 2023 saw the start of the Horizon Europe funded D-STANDART project (https://d-standart.eu/), which aims to reduce the experimental effort needed to characterise the fatigue behaviour of large scale structures, through a combination of developing novel test methodologies, and making use of AI-assisted modelling to account for manufacturing defects and difference in lay-up.

3.3. Fatigue Behaviour of Various Bolted Joints in Composites

A. Macovei, J. Meuzelaar, T. Janssen (GKN Aerospace / Fokker Aerostructures, Papendrecht)

Despite a trend towards more utilization of co-consolidation, welding- and bonding technologies for the assembly of advanced composite structures, a portion of all joints in composites will simply remain using mechanical fasteners for various reasons (accessibility, manufacturing splicing strategies, reparability/removability, out-of-plane loading, electrical bonding etc. etc.). To investigate and compare the performance of various novel (blind) fastener systems in comparison to legacy fasteners and welded joints, GKN Fokker is continuously screening new fasteners in a standardized test configuration using thermoplastic C/PPS laminates, so results can be directly compared to welded joints in the same material.

This standardized single lap-shear test sample is derived from ASTM D5961, but compacted (to save material) and tailored to house two ∅3/16" fasteners of various kinds, see Figure 8. The laminate is a 3.1mm C/PPS pre-consolidated plate from Toray Advanced Composites (5-Harness T300 Carbon Fabric / TC1100), resulting in a D/t-ratio of 1.5-1.6 depending on the exact fastener. This is a very representative joint layout for control surfaces, which is a typical product at GKN. Besides comparison of various (blind) bolt types, the specimen also allows a realistic comparison of important factors in the joint like pre-tension/torque, fastener head/tail style, presence of shims and stiffness of the back-up structure.

Figure 8 Standardized Test Specimen

Most of these tests are static tests, performed at room temperature (to save time and cost) as it is the general experience that most composite structure (including joints) are statically critical in the design. Parameters evaluated are static strength, failure mode, weight and (installed) cost.

To verify the assumption that the static performance of the evaluated fastener systems indeed is a good indication for dynamic behaviour as well, it was decided to expose a group of fastener types to fatigue loading as well. From the large group of tested fasteners, a subset of blind fasteners was selected based on a variability of static failure modes (fastener head failure, blind bulb deformation, bearing failure, pull-through) and their relevance for GKN Fokker. Moreover, a solid, 2-piece fastener system (Hi-Lite) was added as a reference fastener (as solid fasteners generally give the best fatigue performance).

To prevent the need for an anti-buckling guide (which always gives a debate on the amount of friction induced in the specimen), the samples are tested at R = 0.1, i.e. Tension-Tension fatigue. Peak load levels were varied with the aim to obtain a fatigue life of 10^3 – 10^5 cycles for each fastener type. To limit test time, cycling was stopped in case $2x10^5$ cycles were achieved. For these run-out samples, the residual strength was then established in a subsequent static test. The test set-up, as shown in Figure 9, features a thermocouple (monitoring to prevent heat development in the sample) and LVDT (to measure any wear behaviour of the joint).

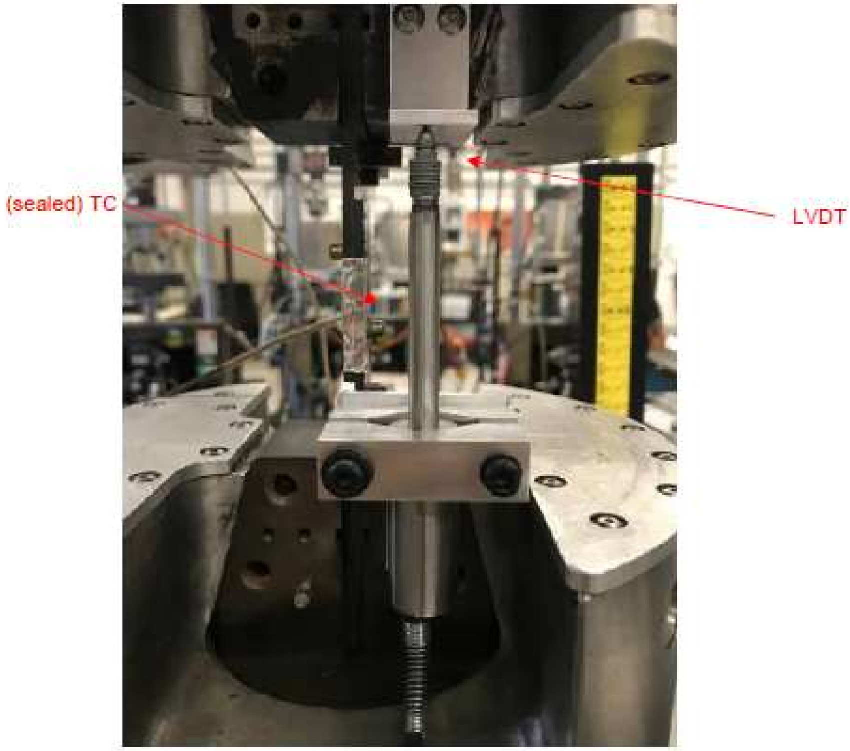

Figure 9 Test Set-up (incl. LVDT and Thermocouple)

During testing, it was found that peak load levels needed to be increased above expectation to prevent all samples reaching test run-out: on average, no noticeable degradation occurred below a peak load equalling 70% of the joint's ultimate static strength. Due to the higher loads, more heat development in the joint was about to occur, so cycling frequencies needed to be reduced to prevent sample overheating. Overall, observed failure modes were identical to that of the static test (generally a combination of modes, see *Figure 10;* only a few samples showed a transfer in failure mode (at high load levels). For the samples reaching test run-out, relatively high residual strengths were measured (77-122% of the static test results); most interesting here are the observed values above 100% (indicating an improvement of static strength during cycling!). Further examination and testing is needed to study this peculiar phenomenon.

Figure 10 Example Failure Mode: Combination of Fastener Head Failure and Tilting/Laminate Bearing

The fatigue performance of all tested fasteners exceeded expectations; relatively high loads could be cycled without failure before $2x10^5$ cycles (depending on fastener type, 48-96% of the static ultimate joint strength could be cycled 200 kcycles without failure). This is partly contributed to the fact that these tests were without the presence of a shim, which typically reduces mechanical joint performance, especially in fatigue (experience from other tests at GKN Fokker), so care should be taken when extrapolating these result to other joint configurations. Failure modes per fastener type obtained in fatigue matched very well with the previous static tests, confirming the relevance of static testing for the bolted joints.

As could be expected, the fasteners with static failure modes in the composite performed better in fatigue than fastener types with fastener-dominated static failure modes. Moreover, on the fastener pre-tension a general positive trend has been observed for the relation between a longer fatigue life and higher pre-tension (stronger effect than observed during static testing).

Acknowledgements: this research was partly funded by European project Cleansky 2. Moreover, fastener manufacturers Howmet, Monogram, Cherry and Lisi are recognized for their delivery of fastener test samples.

3.4. Damage tolerance approach for thermoplastic orthogrid fuselage

Jan E.A. Waleson and Jaap Willem van Ingen (GKN Aerospace / Fokker Aerostructures)

Integral thermoplastic orthogrid structure is proposed as a light, cost competitive option for a non-pressurized, double curved aft fuselage structure of a business jet. See figure 1 and [10]. Drag reduction using the area rule for the fuselage between the engines led to the double curved shape, which is more easily realized in composites. The structure consists of a co-consolidated skin, laid up by automated fiber placement, and flat pre-forms for the frames and stringers. The joints that are mainly loaded in shear are made by means of short-fiber fillets in so-called “butt joints” and conduction welding. Use of mechanical fasteners is limited to panel joints and joints to metal structure. The question to be answered was how the damage tolerance of such a disruptive, highly integrated thermoplastic fuselage structure might be proven or enhanced.

Advisory Circular AC20-107B, ref. [11], is used as conclusive damage tolerance approach based upon detectability, inspection interval, and residual strength of the different damage categories.

The damage resistance of the structure is tested to determine the damage scenario and detectability for each of the following damage categories: barely visible impact damage (BVID), visible impact damage (VID), and obvious damage. Allowable manufacturing defects are covered by the impact damage. Subsequently, the damage tolerance is assessed by analysis supported by test, which enhances insight and reduces costs.

Damage tolerance for the different damage categories was assessed for impacts on the inside of the structure next to the skin-stringer butt joints and on the stringer caps and for impacts on the outside of the structure at the stringers, between the stringers, and at the frames.

No showstoppers were found in the extensive work.

As an extra layer of safety arrest of a large notch (two half bays) with failed stringer is being tested and analysed at NLR, as structural damage capability, which is at the discretion of the OEM. To enhance the residual strength, local plies in the stringer direction were added to the skin layup.

The positive results prove that integrated, cost competitive structure can be designed damage tolerant and safe.

Figure 11 New stiffened fuselage panel concept without mechanical fasteners.

3.5. Durability of thermoplastic welded joints

Jan E.A. Waleson (GKN Aerospace / Fokker Aerostructures), Hugo Boutin (Rescoll), Maarten Labordus (KVE Composites)

Part of the Clean Sky 2 STUNNING / MECATESTERS project covered mechanical fatigue, environmental stress cracking, and so-called ratcheting at hygro-thermal cycling of Ca/PEKK thermoplastic conduction welded joints. During ratcheting stresses in the matrix are increasing due to viscoelastic relaxation of the matrix [12]. Welded single lap shear specimens were used for all tests. The mechanical fatigue tests were delayed.

Figure 12 shows the effect of environmental stress cracking: how the load that the weld can carry drops as a function of time of sustained loading and submersion in the acid mixture of Skydrol and water.

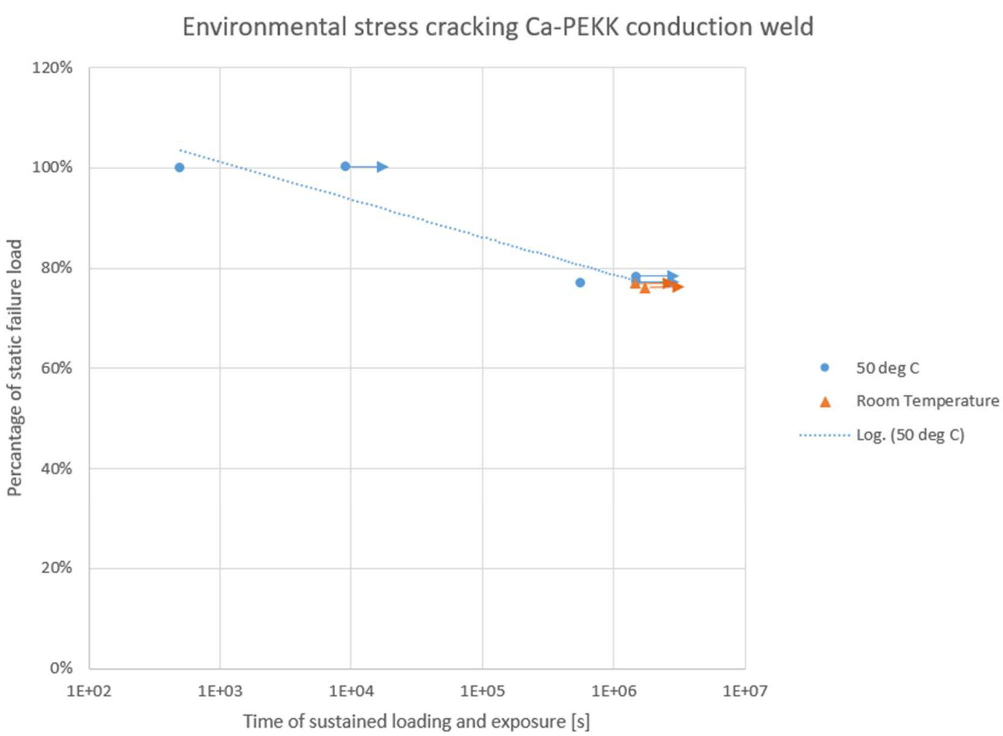

Figure 12 Drop of failure load as a function of time of sustained loading and submersion in a mixture of Skydrol and water.

The 60 hygro-thermal cycles to test ratcheting were as follows:

1. Temperature decrease at the dry condition (96°C / 10% RH → 60°C / 10% RH);
2. Moisture absorption at 60°C / 85% RH (60°C / 10% RH → 60°C / 85% RH);
3. Temperature increase at the wet condition (60°C / 85% RH → 96°C / 85% RH);
4. Moisture desorption at 96°C / 10% RH (96°C / 85% RH → 96°C / 10% RH).

In the 2nd-29th and 31st-59th cycles full absorption and full desorption was not aimed for, but the intervals were instead shortened to 24 h.

The cycles were similar to the ones that caused ratcheting in thermoset spliced, co-cured specimens at NIAR.

Figure 13   Measurement of the curvature of a cross-ply after one of the long cycles.

No significant effect on the strength of the welded single lap shear specimens was found. Besides, the curvature of cross-plies (figure 2) did not significantly increase as a function of the number of cycles, as was observed at the thermoset specimens at NIAR. The Ca-PEKK laminate and welded joint did not show the sensitivity to ratcheting as observed for the thermoset spliced specimens at NIAR.

The research was made possible through funding by the Clean Sky initiative through the call JTI-CS2-2018-CfP08-LPA-02-25 “Micro mechanical characteristics of a PEKK Co-consolidation/welded joint for use in thermoplastic fuselages”, which has been granted to KVE Composites and Rescoll, with GKN Aerospace / Fokker Aerostructures as topic manager.

4. Prognostics & Risk Analysis

4.1. Uncertainty Quantification of the lifetime of Self-Healing Thermal Barrier Coatings

Anuj Kumthekar, Sybrand van der Zwaag, Sergio Turteltaub (TU Delft), Sathiskumar A. Ponnusami (City University London)

In this study, thermal cyclic behaviour of self-healing thermal barrier coatings (SH-TBC) was analysed numerically to develop a lifetime prediction model [13]. The objective of the detailed modelling and simulation of Self-Healing Thermal Barrier Coatings (SH-TBC) is to extend lifetime of TBCs in jet engines, as illustrated in Figure 14. The self-healing is analysed through parameters like the crack filling ratio and strength recovery, to characterise the evolution of crack patterns and the number of cycles to failure,.

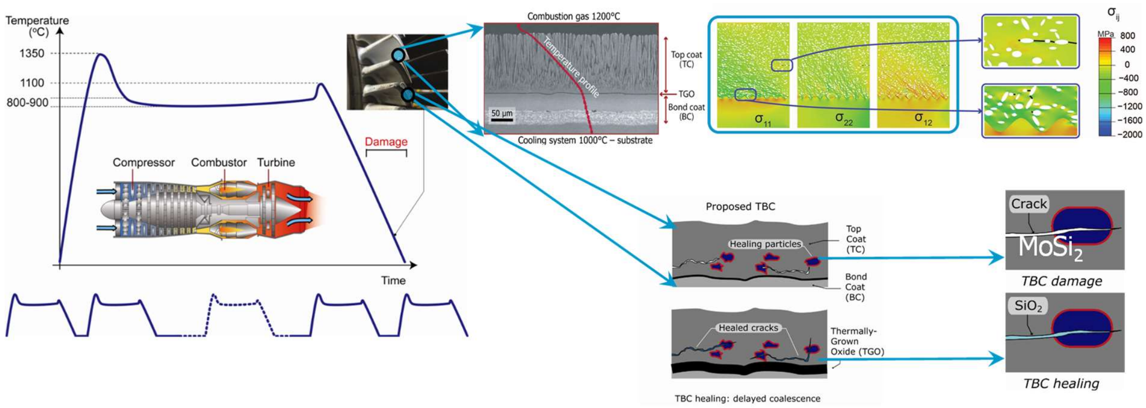

Figure 14 Illustration of growth of oxide layer in thermal barrier coatings (TBC) and cyclic damage due to high thermal stresses during cooling and mismatch in CTE in jet engines (top) and the concept of Alumina-coated $MoSi_2$ self-healing particles embedded in a TBC to heal cracks upon thermal cycling.

In addition, surrogate modelling of SH-TBC lifetime using Polynomial Chaos Expansion were developed to quantify the uncertainties in fracture behaviour and life time of the SH-TBC system, see Figure 15 [14].

This study demonstrated that the sensitivity analysis and optimization of SH-TBC systems results in a quantified increase in lifetime due to self-healing particles, but that it also leads to an increase in scatter in the thermal fatigue life.

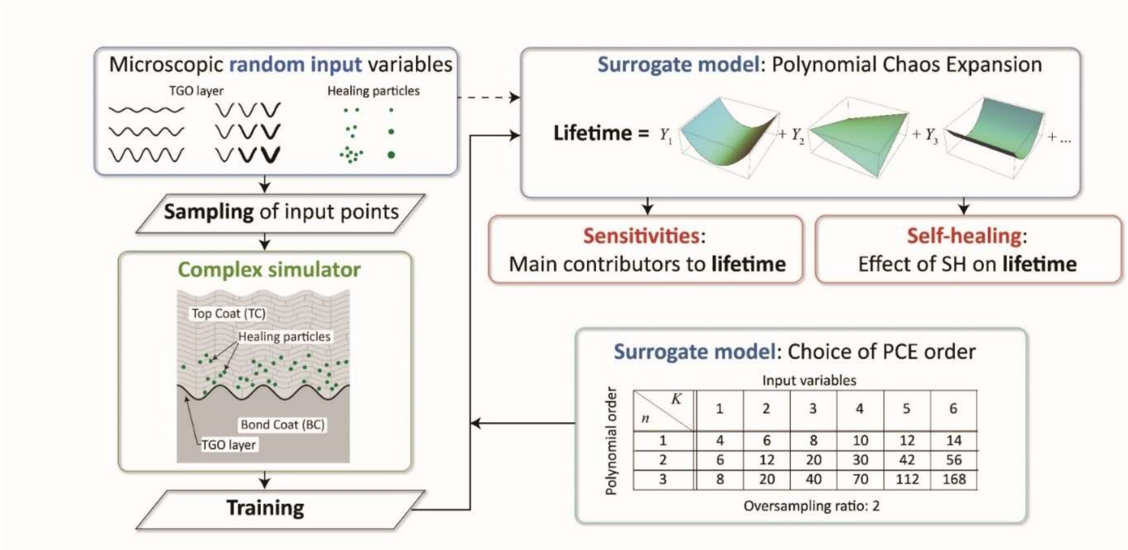

n \ K	1	2	3	4	5	6
1	4	6	8	10	12	14
2	6	12	20	30	42	56
3	8	20	40	70	112	168

Figure 15 Illustration of the surrogate model through Polynomial Chaos Expansion.

5. Non-Destructive Evaluation

5.1. Development and evaluation of various Non-Destructive Inspection techniques at NLR

Jason Hwang, Patrick Jansen, Jacco Platenkamp (Royal Netherlands Aerospace Centre NLR)

Inspection of rotary wing blade can be laborious work. NLR has developed an Automated Rotor Blade Inspection (ARBI) system, which uses multi-domain contactless non-destructive inspection methodologies to identify defects in the structure. Thermography, shearography and 3D optical measurements in combination with a robotic bench allow for extensive automation of the inspection process. Furthermore, the possibility to use automatic defect recognition is being employed. Figure 16 shows the demonstration of this concept on a composite wing (Pipistrel electric aircraft of NLR).

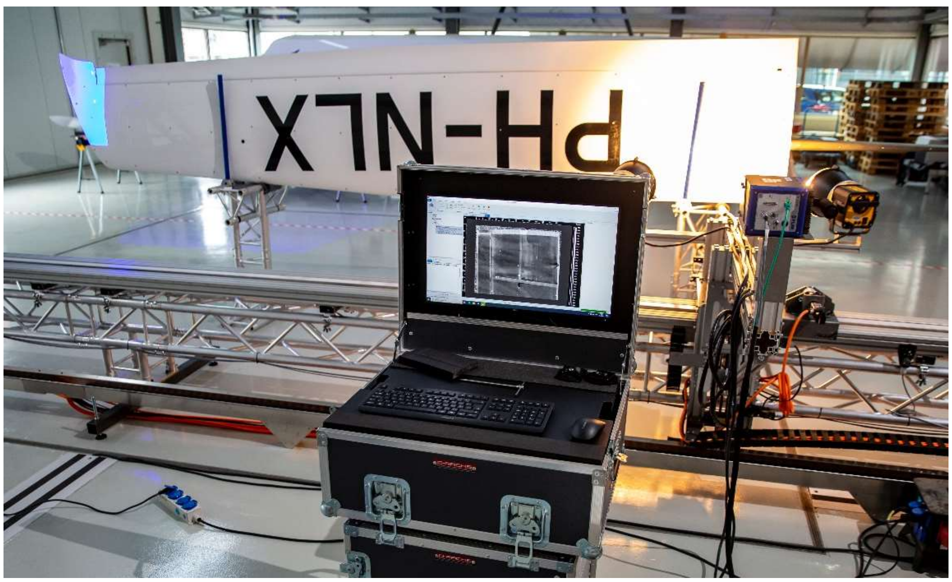

Figure 16 Demonstration of ARBI concept on a composite wing structure.

In order to increase sustainable energy production in the Netherlands, off-shore wind farming is rapidly growing. It is foreseen that the inspection of wind turbine blades has to be automated to anticipate the shortage of labour. A national research programme dubbed Automated Inspection and Repair of wind Turbine Blades (AIRTuB), in which NLR, TU Delft and TNO participate among other partners, has started to address this challenge. A drone with a compact laser line scanner is demonstrated, showing that it is possible to detect surface erosion which can lead to annual energy production loss up to 2%. Furthermore, a miniature crawler is developed to demonstrate the possibilities to inspect for delaminations in the wind turbine blade skin. Figure 17 shows these demonstrators.

Figure 17 Final demonstration of AIRTuB program. Left: drone equipped with a miniaturized laser line scanner. Right: ultrasonic inspection performed with a crawler.

The inspection of aircraft structure under low-observable coatings imposes high downtime because it often requires the removal and repair of the coating. This problem is addressed in the project Advanced Low Observable Coating and Aircraft Structures (ALOCAS). In this project, an Eddy Current array method is evaluated for use on a hybrid structure with LO coating, see Figure 18. The results show that, even with the LO coating, the defects can be detected, albeit with reduced sensitivity.

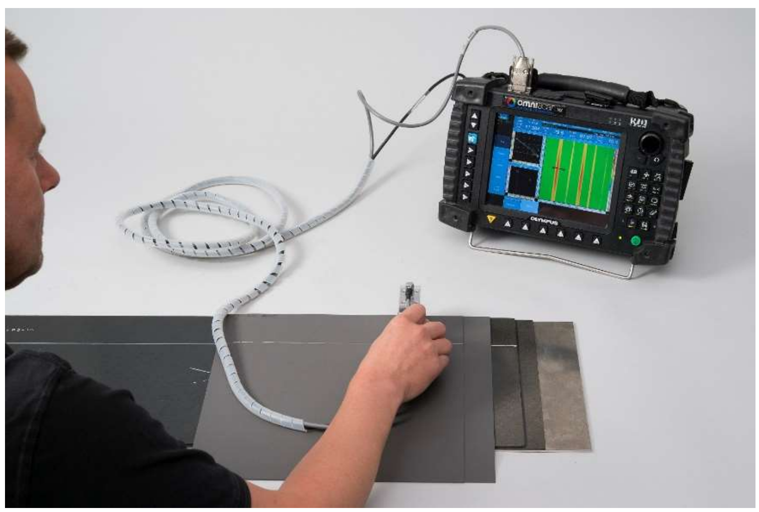

Figure 18 Evaluation of Eddy Current array method on an aluminium specimen with EDM notches and flat bottom holes (simulating corrosion). Various combinations of CFRP skin thickness and LO coating have been tested.

5.2. Impact detection and localisation

Frank Grooteman, Jan Willem Wiegman (Royal Netherlands Aerospace Centre NLR)

A significant part of the aircraft maintenance effort is formed by scheduled inspections of the airframe and mechanical systems. Modern technologies such as fibre optic based SHM (Structural Health Monitoring) and data driven PHM (Prognostic Health Management) are the key to more efficient maintenance strategies such as Predictive Maintenance or Condition Based Maintenance. For composite aircraft structures, mechanical impact events on the ground, during take-off, flight or landing are a main source of damage. An SHM sensor network that can detect such an impact event and determine the impact location, from the sensor responses measured during the impact, can already significantly alleviate the inspection burden by providing guidance to an inspector, when and where to inspect the aircraft structure, thereby significantly improving the efficiency and accuracy of inspections.

Impact tests of various energy levels and at various locations have been performed at NLR on a stiffened thermoplastic horizontal tail plane in the TAPAS2 project (Figure 19) and a composite engine Nacelle of Spirit AeroSystems in the EU SuCoHs project (Figure 20). The tests were executed to demonstrate the capability of optical fibre Bragg grating (FBG) sensors for this kind of SHM application. The main goal was to demonstrate impact event detection and localisation with FBGs. Other objectives were to demonstrate that strains can be accurately measured with FBGs for a large structure and at low load levels for load and usage monitoring.

The impact tests on both structures (and others) demonstrated that large areas of complex composite aircraft components can be successfully monitored for impact events and the impact location can be derived from the FBG strain responses of a limited number (six to eight) of optical FBG sensors. A number of examples are depicted in Figure 19 and Figure 20, where the blue dots are the sensor locations, the green dot the impact location and the red dots the computed impact location. Furthermore, it was demonstrated that higher sample rates (20 kHz for horizontal tail plane and 100 kHz for the Nacelle) yield more accurate localisation results.

Current research activities are to examine if a threshold impact energy level (force reconstruction) or even the presence of damage can be derived from the same measured response signals, to further determine the need for an inspection. Depending on the already known location, an impact energy threshold will tell the probability of damage to be present after the impact and whether an inspection is required. This is even better, if the presence of damage can be derived reliably.

Figure 19 Impact localisation with FBGs on a stiffened thermoplastic horizontal tail plane.

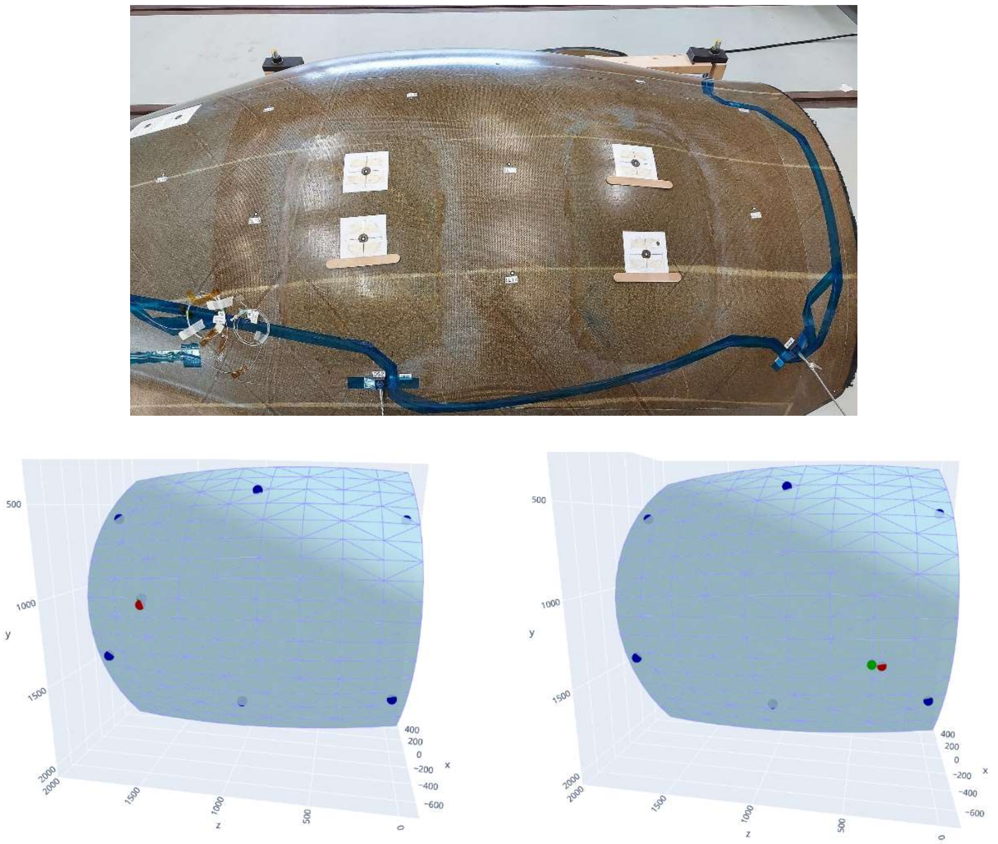

Figure 20   Impact localisation with FBGs on a Spirit AeroSystems composite engine nacelle.

6. Structural Health & Usage Monitoring

6.1. Dynamic continuous fiber optical strain sensing for damage diagnosis on beam-like composite structures

Irene Solbes Ferri, Saullo G. P. Castro, Roger M. Groves (TU Delft), Johannes Knebush, Yves Govers (DLR)

The objective of this master project [15] is to improve the current SHM techniques for global damage identification of beam-like composite structures. The studied damage diagnosis method is based on structural vibrations from which the modal parameters are obtained. The literature study provides an overview of the most common vibration-based damage identification methods. The modal curvature shape- and modal strain energy-based methods are selected due to their higher sensitivity to local damages. These methods are applied on an aero-elastically tailored composite wing. High-spatial-resolution modal shapes are extracted from the structure with a state-of-the-art fibre optic strain sensing technology based on Rayleigh back-scattering. Damages are simulated in the wing employing localized mass attachments. The achievable level of damage identification with this technique is found and characterized. The different vibration-based methods are compared and their potential is discussed. It is concluded that the used sensing technique is an excellent choice for global damage diagnosis in composite structures.

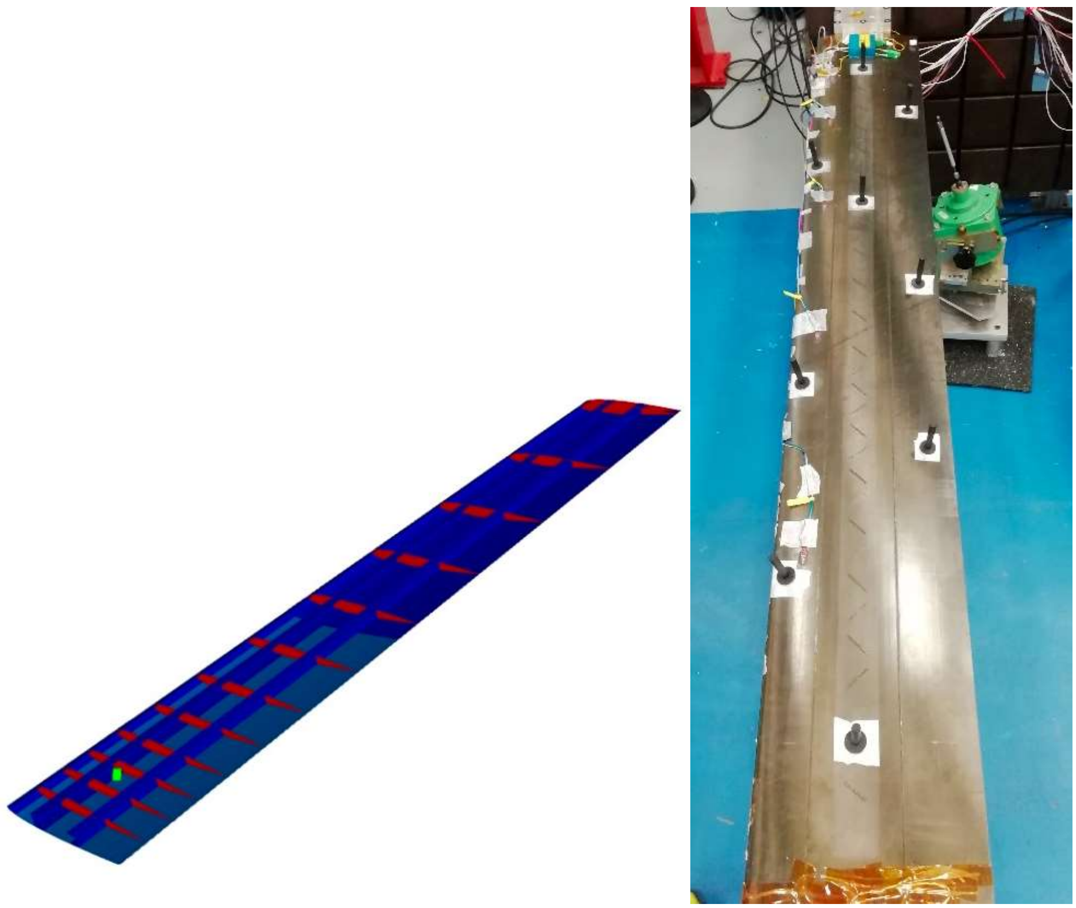

Figure 21 Isometric view of the wing model in NASTRAN: ribs and spares lay-out (left) and illustration of experimental test article (right)

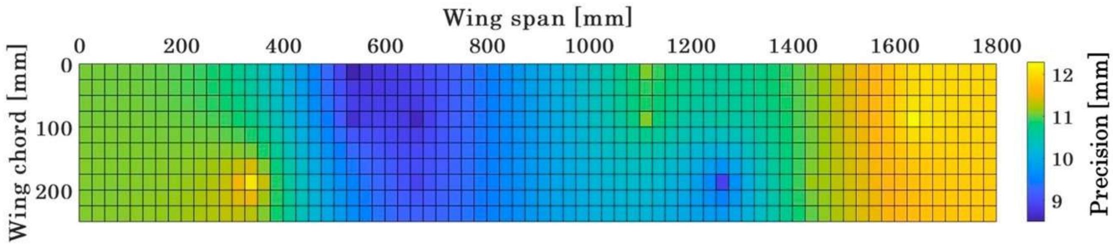

Figure 22 Damage location precision map

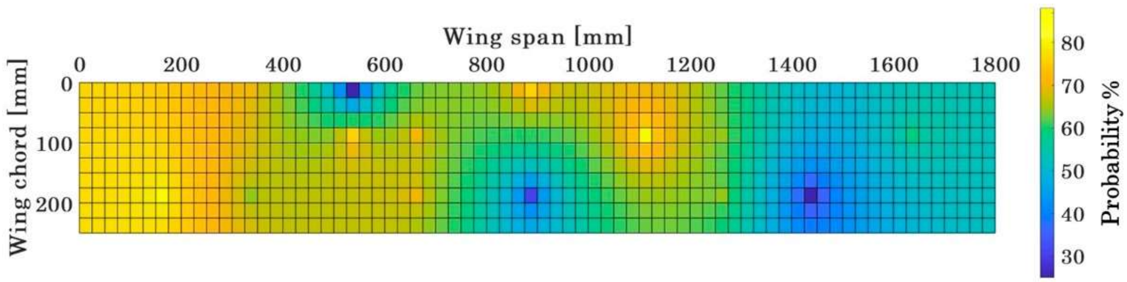

Figure 23 Probability map of correct damage location

6.2. Shape Sensing and Load Reconstruction for Static and Dynamic Applications

Paolo Minigher, Saullo G. P. Castro, Janto Gundlach (TU Delft)

The reconstruction of the elastic deformed shape of a structure from strain measurements is a field which has received considerable attention over the years. This work [16,17] aims to suggest some improvements for wing-like structures trying to limit as much as possible the amount of strain measurements needed. A simple beam model is proposed based on the framework of the inverse Finite Element Method (iFEM). Then, the performances of iFEM using shell elements will be enhanced pre-extrapolating the strain field and the results will be compared with another shape sensing method, the so-called Modal Method (MM). In the final part of the work the external loads under the form of a pressure field are recovered using either the reconstructed displacements and directly the strain measurements. Static and dynamic analyses will be carried out, so recovering the load both in space and in time. The results obtained show that the beam model developed allows to obtain a satisfactory bending reconstruction of the structure, while the twist is not always accurate. Computing the full displacement field with iFEM brings to a relatively good representation, even though not as satisfactory as the one delivered by the Modal Method. Finally, recovering the static external loads directly from the strain measurements seems to perform better compared to the reconstruction from the full displacement field, but it is significantly affected by noise and uncertainties. The dynamic load reconstruction is in general much more challenging, and the results obtained often show a significant error compared to the reference solution.

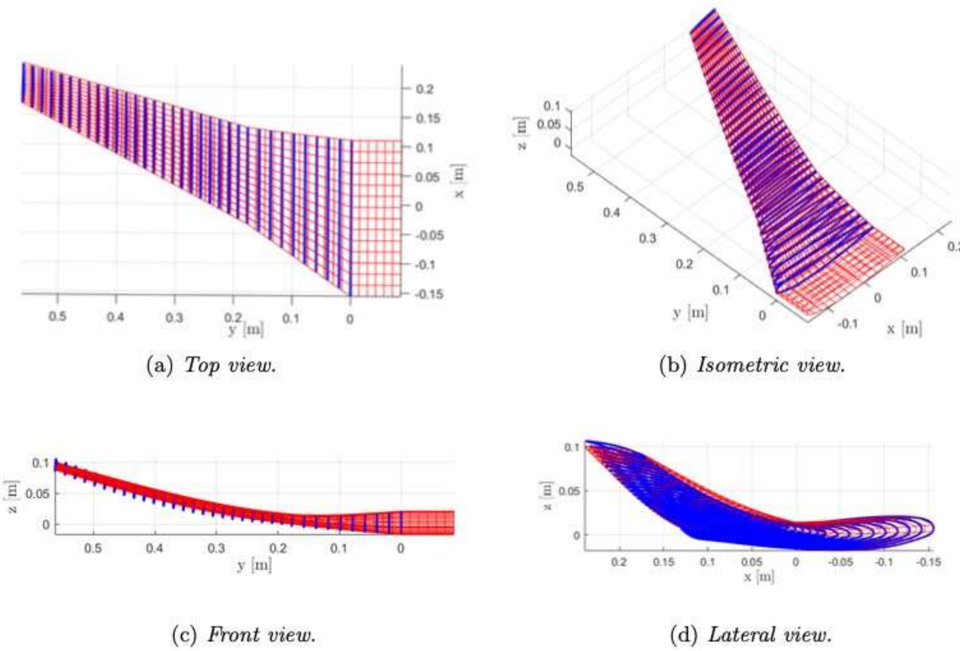

(a) *Top view.* (b) *Isometric view.* (c) *Front view.* (d) *Lateral view.*

Figure 24 Reconstructed deflection (blue line) and reference deformed shape (red mesh) for constant pressure case.

7. Fleet Life Management

7.1. Individual tracking of RNLAF aircraft

Marcel Bos (Royal Netherlands Aerospace Centre NLR)

The Royal Netherlands Air Force (RNLAF) and NLR collaboratively keep track of the loads and usage of most aircraft types in the RNLAF inventory, viz. the F-16 Block 15, C-130H/H-30, NH90, AH-64D, ICH-47D and ICH-47F. This is done on an individual basis (individual aircraft tracking, IAT) and involves the installation of data acquisition and recording equipment, the development of modern data information systems and processing software, the development of fatigue and/or corrosion damage indices, the collection and processing of loads and usage data, the fusion of the collected usage data with the maintenance databases of the RNLAF to enable and enhance reliability analyse efforts, and the reporting of the processed data to the RNLAF. The results are used to:

- keep track of the consumed fatigue life;
- assess the severity of specific missions and mission types;
- evaluate and possibly optimize the usage of the fleets;
- optimize maintenance programs;
- assess/anticipate required structural modifications programs;
- provide the OEM with high-quality data in case of modification programs;
- rationalise decisions regarding tail number selection in the case of out-of-area deployment, fleet downsizing, decommissioning, etc.;
- develop load spectra for full-scale component testing;
- gain insight in the root causes of accidents and failures;
- enhance reliability analyses.

Many details of these programs were already supplied in previous National Reviews. A new activity is the development of a Fibre Optic Sensing-based IAT-program for the Apache AH-64E helicopter that is currently being introduced in the RNLAF. This is done in collaboration with the Boeing company.

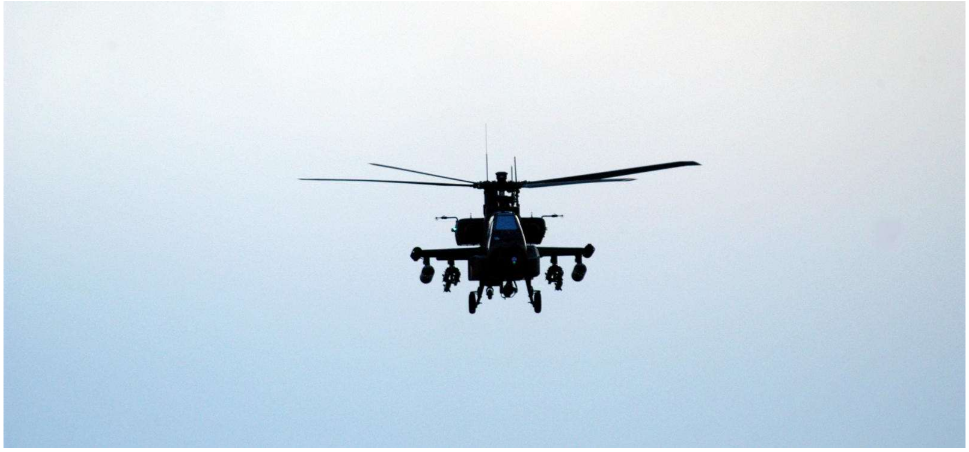

Figure 25 AH-64E Apache helicopter of the RNLAF (from: NLR repository).

8. Special Category

8.1. Milestone Case Histories in Aircraft Structural Integrity

Russell Wanhill (NLR), Simon Barter, Loris Molent (DST-G)

Although there are increasing uses of innovative materials in aircraft structures, particularly the increasing use of composites during the last 3-4 decades, the evolution of aircraft structural integrity since the early 1930s has been concerned largely with the service behaviour of high-strength metallic materials, particularly aluminum alloys for both civil and military airframes, high strength steels for landing gears and other high load density components, and titanium alloys mainly, but not entirely, for heat-resistant sections and components surrounding and supporting the engines.

Service failures, especially accidents, have greatly influenced this evolution. Four case histories are often cited: the De Havilland Comets (1954), General Dynamics F-111A (1969), Boeing 707 cargo (1977), and a Boeing 737 (1988). We have added two more that have also made significant (milestone) contributions: Boeing B-47Bs and Es (1958), and an Aermacchi MB-326 H (1990).

Schematics of the ways in which these milestone case histories have influenced aircraft fatigue and fracture changes are given in Figure 26 and Figure 27.

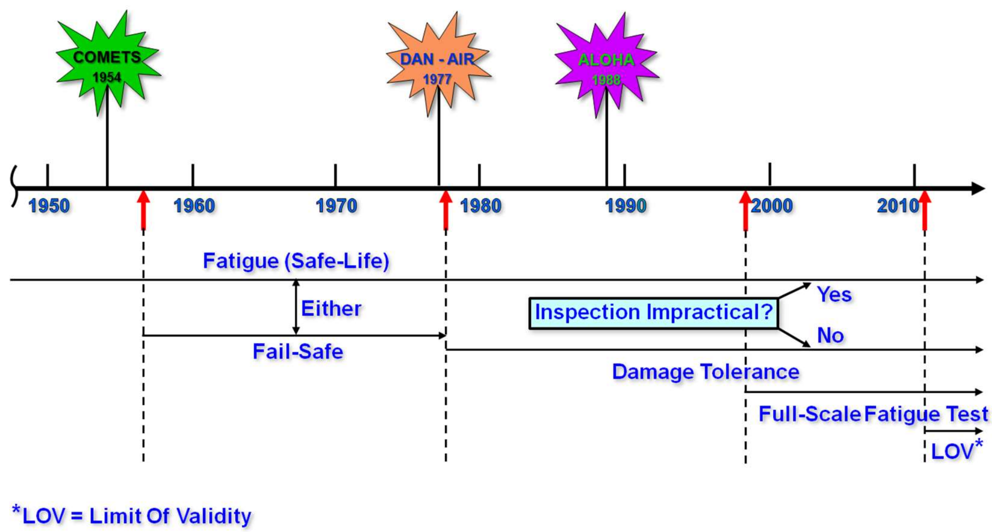

Figure 26 Milestone civil aircraft accidents causing fatigue and fracture requirement changes

These milestone case histories are discussed in detail, including the lessons learned and the developments in fatigue analysis stimulated by them, in [18]. In addition, the significance of short fatigue cracks, the relations between corrosion and fatigue, and ongoing material developments, especially composites, are briefly discussed with respect to their broad implications for structural integrity.

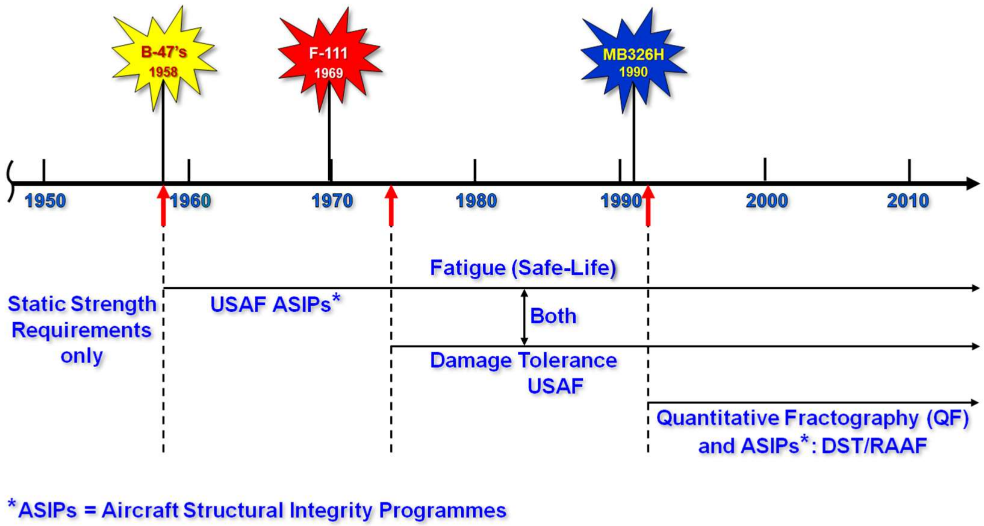

Figure 27 Milestone military aircraft accidents causing fatigue and fracture requirement changes: DST = Defence Science and Technology (group): RAAF = Royal Australian Air Force.

8.2. The lead crack concept history 30 years on

Russell Wanhill (NLR), Simon Barter, Loris Molent (DST-G)

Since the early 1990s extensive quantitative fractography (QF) of early nucleation and growth of airframe fatigue cracks that have resulted in accidents, or led to threats to structural safety, have shown that the largest or "lead" cracks often show approximately exponential growth. These observations have been formalised in the lead crack concept and development of the Lead Crack Fatigue Lifing Framework (LCFLF) [19-21]. This has now progressed to a stage where it provides a robust and appropriately conservative method of assessing crack growth, enabling the setting of inspection and maintenance periods for a variety of in-service aircraft fatigue cracking problems. The framework has been used extensively in airframe life predictions and or life extensions by numerous airworthiness authorities.

The LCFLF relies on determining the equivalent crack-like sizes of the fatigue-nucleating discontinuities and the crack depths at known points in the fatigue lives. This method is flexible in that it may be pragmatically combined with fracture mechanics models of crack growth, provided they have been verified by actual measurements [21].

This paper summarises the current knowledge state for the LCFLF and provides some new examples of the framework directed at determining the crack growth history from limited quantitative fractography or in-service crack length measurements. It has increasingly become an important tool for aircraft sustainment and fatigue failure analyses.

References

[1] Quan H (2022), *The energy dissipation during fatigue crack growth.* PhD dissertation https://doi.org/10.4233/uuid:5c4d7f24-4df6-40b2-b58f-8f673f17ae4c.

[2] Quan H, Alderliesten RC (2022), The energy dissipation during fatigue crack growth in metallic materials, Eng Fract Mech 269, https://doi.org/10.1016/j.engfracmech.2022.108567

[3] Van Kuijk JJA (2022), *Novel insights into the physics of fatigue crack growth: Theoretical and experimental research on the fundamentals of crack growth in isotropic materials.* PhD dissertation https://doi.org/10.4233/uuid:a7676dc2-8003-4495-839d-b900f95fd061.

[4] Pascoe JA (2021), Slow-Growth Damage Tolerance for Fatigue after Impact in FRP Composites: Why Current Research Won't Get Us There. Theor. Appl. Fract. Mech. 116, 103127, doi:10.1016/j.tafmec.2021.103127.

[5] Biagini D, Pascoe JA, Alderliesten RC (2023), Investigation of Compression after Impact Failure in Carbon Fiber Reinforced Polymers Using Acoustic Emission. J. Compos. Mater. 0, 002199832311638, doi:10.1177/00219983231163853.

[6] Biagini D, Pascoe JA, Alderliesten RC (2022), Experimental Investigation of Fatigue after Impact Damage Growth in CFRP. Procedia Struct. Integr. 42, 343–350, doi:10.1016/j.prostr.2022.12.042.

[7] Cameselle-Molares A, Vassilopoulos AP, Keller T (2018), Experimental Investigation of Two-Dimensional Delamination in GFRP Laminates. Eng. Fract. Mech. 203, 152–171, doi:10.1016/j.engfracmech.2018.05.015.

[8] Van der Panne M, Pascoe JA (2022), Fatigue Delamination Growth - Is UD Testing Enough? Procedia Struct. Integr. 42, 449–456, doi:10.1016/j.prostr.2022.12.057.

[9] Alderliesten RC (2018), Fatigue Delamination of Composite Materials - Approach to Exclude Large Scale Fibre Bridging. IOP Conf. Ser. Mater. Sci. Eng. 388, doi:10.1088/1757-899X/388/1/012002.

[10] Van Ingen JW (2016), Thermoplastic Orthogrid Fuselage Shell, Sampe Journal. 52(5): 7-15.

[11] U.S. Department of Transportation, Federal Aviation Administration, Advisory Circular 20-107B, Change 1, Composite Aircraft Structure, August 24 (2010).

[12] Rothschilds RJ, Ilcewicz LB, Nordin P, Applegate, SH (1988), The effect of hygrothermal histories on matrix cracking in fiber reinforced laminates. Journal of engineering materials and technology, vol. 110, 158-168.

[13] Krishnasamy J, Ponnusami SA, Turteltaub S, Van der Zwaag S (2021) Thermal cyclic behavior and lifetime prediction of self-healing thermal barrier coatings, International Journal of Solids and Structures, Article Number111034 https://doi.org/10.1016/j.ijsolstr.2021.03.021

[14] Kumthekar A, Ponnusami SA, Van der Zwaag S, Turteltaub S, (2022) Uncertainty quantification of the lifetime of self-healing thermal barrier coatings based on surrogate modelling of thermal cyclic fracture and healing, Materials & Design, Article Number110973, https://doi.org/10.1016/j.matdes.2022.110973

[15] Irene Solbes Ferri (2022), Dynamic continuous fiber optical strain sensing for damage diagnosis on beam-like composite structures, MSc thesis Delft University of Technology http://resolver.tudelft.nl/uuid:a0bd1c6a-5cca-46ce-bd31-56673dac4024

[16] Paolo Minigher (2022), Shape Sensing and Load Reconstruction for Static and Dynamic Applications, MSc thesis Delft University of Technology http://resolver.tudelft.nl/uuid:7400c81a-c5bf-4422-bc2b-c5870dae46f6

[17] Paolo Minigher, Janto Gundlach, Saullo G. P. Castro, Yves Govers (2022). Shape Sensing with Sparse Strain Information for Aerospace Applications. Preprint. www.doi.org/10.31224/2546

[18] Wanhill RJH, Molent L, Barter SA (2023), Milestone Case Histories in Aircraft Structural Integrity, Comprehensive Structural Integrity, 2nd Edition, to be published in 2023 by Elsevier Ltd: doi:10.1016/B978-0-12-822944-6.00001-3
[19] Molent L, Barter SA, Wanhill RJH (2010) The lead crack fatigue lifing framework, DSTO Research Report DSTO-RR-0353, DSTO Defence Science and Technology Organisation, Fishermans Bend, Victoria 3207, Australia.
[20] Molent L, Barter SA, Wanhill RJH (2011) The lead crack fatigue lifing framework, International Journal of Fatigue, 33: 323-331.
[21] Wanhill RJH, Molent L, Barter SA (2019) Fatigue Crack Growth Failure and Lifing Analyses for Metallic Aircraft Structures and Components, SpringerBriefs in Applied Sciences and Technology, Springer Nature B.V., Dordrecht, The Netherlands.